Flat Spots: Topological Signatures of an Open Universe in Cosmic Background Explorer Sky Maps

Janna J. Levin,[1] John D. Barrow,[1,2] Emory F. Bunn,[1,3] and Joseph Silk[1]

[1]*Center for Particle Astrophysics, University of California—Berkeley, Berkeley, California 94720-7304*
[2]*Astronomy Centre, University of Sussex, Brighton BN1 9QH, United Kingdom*
[3]*Physics and Astronomy Department, Bates College, Lewiston, Maine 04240*

We investigate the behavior of light rays in an open universe with a partly periodic horn topology. The geodesics can be solved exactly and the periodic topology creates characteristic new effects in temperature maps of the microwave background. Large flat regions appear in Cosmic Background Explorer sky maps even when multiple images of astronomical sources are unobservable. [S0031-9007(97)03689-2]

Despite the appeal of a nearly flat cosmology, the universe may have a significant negative curvature. Detailed studies have begun to compare the predicted large-scale structure of open universes with observations [1–4]. We can also learn about the global topology of space from such a comparison. The topology is not directly determined by the matter content of the Universe: indeed, it is not fixed by the Einstein equations at all. Yet, astronomical observations are influenced by the topology of the Universe and the cosmic microwave background radiation (CBR) provides a uniquely sensitive probe. We present some new observable topological effects on the CBR that occur in open universes with nonstandard topologies. These effects can be observed in the absence of ghost images.

The topologies of a flat universe are very limited and have been studied by many authors [5–8], of whom Gott has also considered multiply connected closed and open cosmological spaces. Negatively curved spaces can support a richer spectrum of possible topologies. Negatively curved spaces create hyperbolic geodesic motions. When the space is compactified these trajectories mix and fold, creating a structurally stable chaotic motion [9]. Therefore there are no analytic solutions for the motions of the CBR photons. However, potentially generic features of compact universes may appear in the statistics of ghost images in the CBR [10]. By contrast, if some dimensions are compact while others remain unbounded, the motion may be integrable with exact solutions that display the effects of the compact directions on local geodesics. We consider noncompact topologies of this integrable variety, motivated by the simplicity of regular motion and the strong observable features that they create. We find exact solutions for the geodesic motions on an open space with the topology of a horn [11].

Limits on any universal topology's periodicity scale are often set by searching for periodicity in observations of large structures [5]. Stevens, Scott, and Silk [7] pointed out that, in a flat 3-torus universe, a much stronger lower bound could be set using the CBR power spectrum. The compact space imposes a mode cutoff, which is not observed, and constrains the minimum periodicity scale to exceed the particle horizon. Anisotropic 3-tori were ruled out in Ref. [8]. In an open horn topology there is also a cutoff in two directions but none along the horn. The power spectrum is suppressed but not so dramatically as in the flat 3-torus universe. More prominent features result from suppression of the power spectrum along the narrowest part of the horn. This occurs even if the topology scale is so large that no periodicity of images is visible. We will show that this suppression leads to flat spots in CBR sky maps. However, chaotic geodesic mixing has been avoided at the cost of destroying both homogeneity and isotropy. Only the largest modes are affected since only these will probe the topology scale. Consequently, a contribution to the lowest multipoles of the angular power spectrum is prominent in the maps.

Consider an open Friedmann metric

$$ds^2 = a^2[-d\eta^2 + dr^2 + \sinh^2 r(d\theta^2 + \sin^2\theta\,d\phi^2)].$$

Make the coordinate transformation [11], $e^{-z} = \cosh r - \sinh r \cos\theta$, $e^{-z}x = \sin\theta \cos\phi \sinh r$, $e^{-z}y = \sin\theta \times \sin\phi \sinh r$, so the metric becomes

$$a^{-2}ds^2 = -d\eta^2 + dz^2 + e^{-2z}(dx^2 + dy^2). \qquad (1)$$

The topology is induced by identifying points periodically along x and y by $(x, y) \equiv (x + b, y + h)$, where b and h are constants, to create a 2-torus (two-dimensional torus). This torus is stretched or shrunk by the factor e^{-2z} along the z axis to create a toroidal horn. The comoving proper area of the torus is $e^{-2z}bh$ and depends on location along the z axis. The global topology clearly introduces global inhomogeneity as well as global anisotropy.

Primordial photons scatter off perturbations in the background curvature. In an open universe the Sachs-Wolfe effect, which produces the CBR temperature perturbation $\delta T/T$, receives a contribution from the surface

of last scattering and from a cumulative integral over the gravitational potential taken along a geodesic,

$$\frac{\delta T}{T} = \frac{1}{3}\Phi(\eta_o \hat{n}) + 2\int_o^{\eta_o} d\eta \, \Phi(\eta \hat{n})', \qquad (2)$$

where $' \equiv d/d\eta$. The potential $\Phi(\eta_o\hat{n})$ is to be evaluated somewhere in the volume of last scattering. We need to locate in that volume the sphere of radius η_o we see in direction $\hat{n}(\theta,\phi)$. The most general geodesics can be located [12] but we only need the radial geodesics in spherical coordinates. The periodicity of the manifold will be accounted for by imposing periodic boundary conditions on the eigenfunctions of the potential. We receive light rays along the lines

$$e^{-z} = \cosh(\eta_o - \eta) - \sinh(\eta_o - \eta)\cos\theta,$$
$$e^{-z}x = \sin\theta\cos\phi\sinh(\eta_o - \eta), \qquad (3)$$
$$e^{-z}y = \sin\theta\sin\phi\sinh(\eta_o - \eta).$$

Here, θ and ϕ are angles defining the direction $\hat{n}(\theta,\phi)$ in which the photon is observed. Parametrically, the photon path is $e^{2z} = W_i^{-2} - (x - \hat{x}_i)^2 - (y - \hat{y}_i)^2$. The constants W_i, x_i, y_i can be related to $\hat{n}(\theta,\phi)$ by $W_i^2 = \sin^2\theta$, $\hat{x}_i = \cos\phi\cot\theta$, and $\hat{y}_i = \sin\phi\cot\theta$. If we identify the topology by $(x,y) \equiv (x + b, y + h)$, the photons will spiral around the flat torus in (x,y) while the entire torus is hyperbolically stretched as light moves along z. The most general photon motion will be a looping spiral. Any photon traveling with increasing z eventually hits a maximum and then wraps back. As $W_i \to 0$, the geodesics straighten out. If $W_i^2 = 0$ there is no motion along (x,y) and the trajectories are the lines $z = \pm\eta + z_i$.

The gauge-invariant gravitational potential perturbation, Φ, can be expanded in terms of eigenfunctions $\Phi = \int dk \sum_w \sum_n \Phi_{kwn}(\eta)\psi_{kwn}(x,y,z)$, where the ψ_{kwn} are spatial eigenfunctions and the $\Phi_{kwn}(\eta)$ are the time-dependent amplitudes. The cosmological perturbations satisfy the scalar wave equation $\Phi'' + 2\mathcal{H}\Phi - \Delta\Phi$, with $\mathcal{H} \equiv a'/a$. Following [2], we look for separable solutions with $\Phi_{kwn} = \hat{\Phi}_{kwn}F(\eta)$. The $\hat{\Phi}_{kwn}$ is a primordial time-independent perturbation predicted from, say, inflation; $F(\eta)$ describes the time evolution with

$$F(\eta) = 5\frac{\sinh^2\eta - 3\eta\sinh\eta + 4\cosh\eta - 4}{(\cosh\eta - 1)^3}. \qquad (4)$$

The spatial eigenmodes can be found in the (x,y,z) coordinate system [11]. If

$$\frac{\delta T}{T}(\hat{n}) = \int_0^\infty dk \sum_{wn} \Phi_{kwn}(\eta_o\hat{n})N_{kwn}L_{kwn} \qquad (5)$$

with the normalization

$$N_{kwn} = \left(\frac{2k\sinh(\pi k)}{\pi^2}\frac{(2 - \delta_{w0})(2 - \delta_{n0})}{bh}\right)^{1/2}, \qquad (6)$$

then the spatial eigenfunctions are

$$L_{kwn} = \left[\frac{1}{3} + 2\int_{\eta_i}^{\eta_o} d\eta \, F'(\eta)\right]e^z K_{ik}(Qe^z)$$
$$\times \begin{pmatrix} \sin(\frac{2\pi w}{b}x) \\ \cos(\frac{2\pi w}{b}x) \end{pmatrix}\begin{pmatrix} \sin(\frac{2\pi n}{h}y) \\ \cos(\frac{2\pi n}{h}y) \end{pmatrix}, \qquad (7)$$

where K_{ik} is a modified Bessel function with imaginary index and the entire function is included here in the integration over η. The quantity Q in the argument of the Bessel function is related to the discrete eigenmodes through $Q^2 = 4\pi^2(w^2/b^2 + n^2/h^2)$. The integral is taken from the time of last scattering, η_i, until today, η_o. We have not included the supercurvature modes in the integral in Eq. (5) since they were not found to contribute significantly.

Using the convention of [2], the primordial fluctuation amplitude is assigned an independent Gaussian probability distribution

$$\langle\hat{\Phi}_{kwn}^*\hat{\Phi}_{kwn}\rangle = \frac{2\pi^2}{k(k^2 + 1)}\mathcal{P}_\Phi(k)\delta(k - k')\delta_{ww'}\delta_{nn'}.$$

The prediction of de Sitter inflation is that $\mathcal{P}_\Phi$ is a number. We assume all modes are statistically independent and equiprobable. In a homogeneous universe, the amplitude of perturbations will be the same everywhere, on average. By contrast, in our model the amplitude decays inside the small regions of the horn [11]. Although the amplitude of each mode is assigned a value assuming Gaussian statistics, the global anisotropy may not be Gaussian.

Curvature and topology effect wavelengths long compared to the diameter of the torus in a given direction. The long-wavelength limit is $Qe^z \gg k$, where $K_{ik}(Qe^z) \simeq \sqrt{\frac{\pi}{2Q}}\exp(-z/2 - Qe^z)$. The sum in $\delta T/T$ is quickly suppressed as w and n are increased. The largest contribution to the sum comes from the smallest value of Q. Setting $b = h$ gives a minimum Q value of $2\pi/b$ for $(w = 1, n = 0)$ and $(w = 0, n = 1)$. Consequently,

$$\langle|\delta T/T(\hat{n})|^2\rangle = \frac{2F^2}{9b}\exp[z - (4\pi/b)e^z]\begin{pmatrix} \sin(\frac{2\pi}{b}x) \\ \cos(\frac{2\pi}{b}x) \end{pmatrix}^2$$
$$\times \int_0^{Qe^z} dk \frac{\mathcal{P}_\Phi(k)\sinh(\pi k)}{(k^2 + 1)}$$
$$+ (x \leftrightarrow y) + \dots.$$

For simplicity we have omitted the integrated Sachs-Wolfe term. Along the axis in which the space broadens we have $Qe^{-\Delta\eta} \simeq 0.1$ when $\Omega_0 = 0.3, b = h = 5$. For our approximation to be valid we need $k \ll 0.1$ and only the supercurvature modes are suppressed. The subcurvature modes are mostly unsuppressed and so should produce a normal spectrum in that direction. Along the neck of the horn, however, $Qe^{\Delta\eta} \simeq 13.8$, and so many modes will be affected. From the above expansion the spectrum along the narrow axis of the horn, $\hat{k}$, is suppressed by a factor $\propto \exp[\Delta\eta - (4\pi/b)\exp\Delta\eta]$. For a topology scale of

$b = h = 5$ and a cosmological density parameter of $\Omega_0 = 0.3$ today ($\Delta \eta \simeq 2.398$), the suppression factor is about 10^{-11}. In the narrow part of the horn, the sky temperature map is therefore very much flatter. This suppression is partially camouflaged. Much of the CBR we see originated in the wide part of the horn, traveled down the neck, and wrapped back so that it appears to come from the narrow part of the horn. When we look along the squeezed direction (small θ), the light we see only truly originated in the neck for $\cos \theta \gtrsim (\cosh \Delta \eta - 1)/\sinh \Delta \eta$. For $\Omega_0 = 0.3$ this corresponds to $\cos \theta \gtrsim 0.83$. The rest of the structure seen in that direction is reflected from the wide part of the horn. Like in a hall of mirrors, nothing is where it appears.

On concentric rings centered on the z axis, a range of small k modes will be suppressed when $Qe^z \gg 1$. These rings subtend a half angle in the sky with $\cos \theta > (\cosh \Delta \eta - Q)/\sinh \Delta \eta$, where we have used the geodesic equations (3). The unsuppressed modes give structure on a scale $\lambda(\theta) \lesssim (\cosh \Delta \eta - \sinh \Delta \eta \cos \theta)/Q$. Therefore, we expect to see rings of smaller and smaller lumps as one moves toward the axis. The smaller the topology scale, the smaller the lumps, and the broader the affected patch of sky. If observed, such concentric rings would be further evidence of a universal horn topology, and would also allow us to identify the direction of the horn axis on the sky.

In Fig. 1 we give a predicted Cosmic Background Explorer (COBE) map for $b = h = 1$ and $\Omega_0 = 0.3$. To render the generation of the maps numerically tractable we only sample a finite number of modes. This leads to a completely flat spot where realistically we would expect to see very small structures. When a maximum k is imposed, the flat spot should subtend an angle $\cos \theta \gtrsim (\cosh \Delta \eta - Q/k_{max})/\sinh \Delta \eta$. For the maps shown here, modes up to $k = 10$ are included so that the completely flat spot is predicted to subtend a half-angle of roughly $26°$ for $b = h = 1$ and $\Omega_0 = 0.3$. This agrees with the size of the feature in the top panel of Fig. 1. The small structure on concentric rings discussed above can also be seen most prominently surrounding the spot but the effect extends across half the sky.

The dilution of the power spectrum we have found can be related to an analogous flat space result. In a flat toroidal universe, discrete modes with infinitely small w and n cannot fit inside the finite torus: there is a maximum wavelength $\lambda_{max} = b$ [7]. Similarly, for the open horn-shaped space, there is a long-wavelength mode cutoff in the x and y directions and a suppression of the power spectrum at small k.

For comparison, the angular power spectrum in an anisotropic cosmology is $(2\ell + 1)C_\ell = \sum_m \int d\Omega' \times Y_{\ell-m}(\hat{n}') \int d\Omega \, Y_{\ell m}(\hat{n}) \langle \delta T/T(\hat{n}') \delta T/T(\hat{n}) \rangle$. In the absence of rotational symmetry, the sum over m does not collapse simply. The power spectrum can be estimated by expanding an individual simulated sky map in spherical harmonics and computing the mean-square amplitude
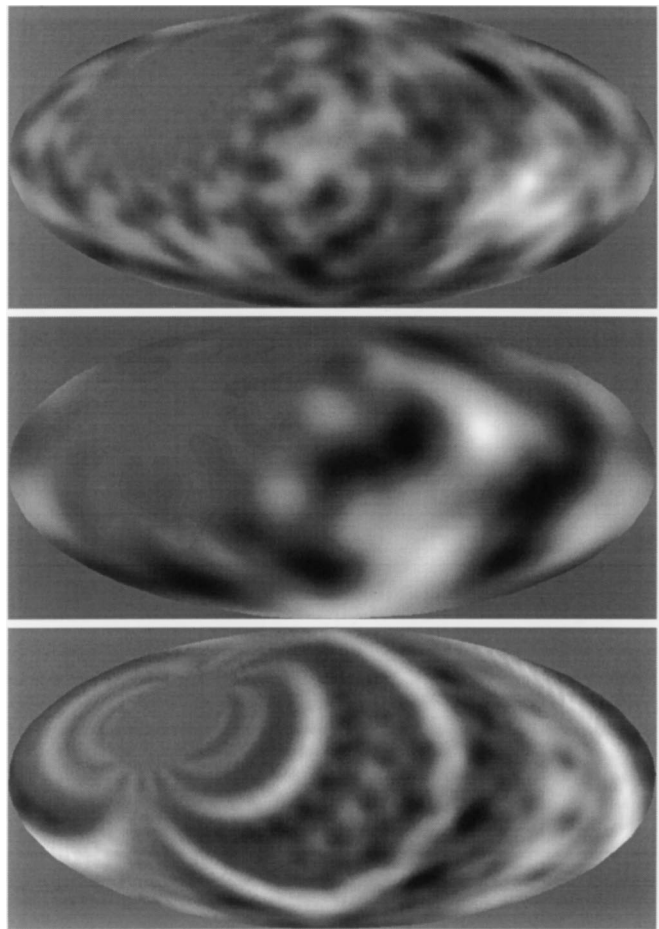

FIG. 1. Three maps of the predicted COBE sky in an open universe wrapped into a horn. The topology scales and cosmic density are $b = h = 1$ and $\Omega_0 = 0.3$ in the top panel. The middle panel has $b = h = 1$ with $\Omega_0 = 0.6$. Asymmetric topology scales $b = 0.3, h = 1$ in an $\Omega_0 = 0.3$ horn lead to an oblong flat spot as seen in the bottom map. When one or both of the scales is small, the temperature variation along z is superimposed on the small fluctuations along x and y.

of the coefficients at a given ℓ. The results of such a calculation are shown in Fig. 2. As can be seen in that figure, the flat region gives a sharp dip in the power spectrum at ℓ's that correspond roughly to the size of the flat spot on the sky. The natural discrete harmonics are also visible in the sequence of dips which follow.

The spectra in Fig. 2 have reductions in power at low ℓ, when compared to a flat Harrison-Zel'dovich spectrum [$C_\ell \propto 1/\ell(\ell + 1)$]. For example, the $b = h = 1$ $\Omega_0 = 0.3$ model has a COBE likelihood roughly 30 times less than that of a flat spectrum. (The likelihood was computed using the Karhunen-Loève method described in [13].) However, there is a great deal more information in these models than just the C_ℓ's: large, coherent structures (flat spots) are predicted that are not seen in the COBE data. Since our models are not described by isotropic Gaussian statistics, we cannot draw precise conclusions from a Gaussian likelihood analysis, but it seems safe to say that these models provide a poor fit to the DMR data.
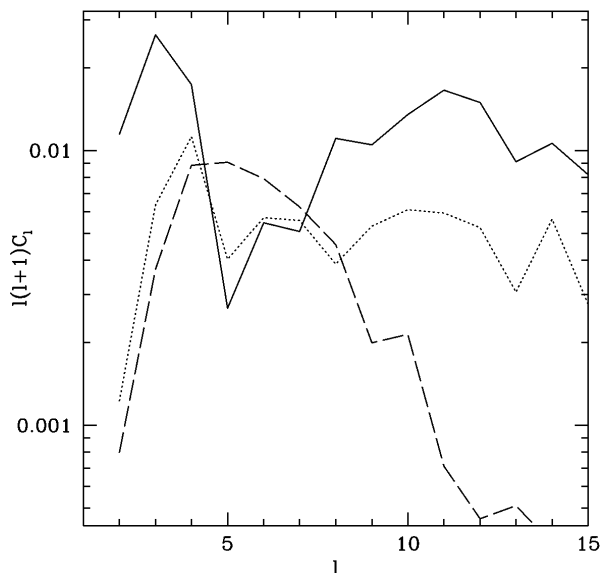
FIG. 2. Angular power spectra. The solid line corresponds to $b = h = 1, \Omega_0 = 0.3$. The dotted line is the asymmetric case of $b = 0.3, h = 1$ and a density of $\Omega_0 = 0.3$ The dashed line depicts $b = h = 1, \Omega_0 = 0.6$. The suppression at higher ℓ as Ω increases is an artifact of the cutoff in the k modes necessary to render the numerical computation manageable.

Topological effects on the geodesics are extremely noticeable even though most trajectories do not wind around the universe more than once. For $\phi = 0$, the maximal number of windings is executed by trajectories in the direction $\cos\theta = \tanh(\Delta\eta)$ for which $m_x = [\Delta x/b] = [\sinh(\Delta\eta)/b] = 1$ for $b = 5$ and $\Omega_0 = 0.3$ (square brackets denote the integer part). Only paths in this vicinity begin to wind more than once. Furthermore, a multiplicity of windings does not guarantee periodicity in this topology. True periodicity requires $x = x + m_x b$ *and simultaneously* that $y = y + m_y h$, where m_x and m_y are the integer winding numbers defined above. The location in the sky, $\hat{n}(\phi)$, of any periodic images can be ascertained by imposing these boundary conditions on Eqs. (3) for fixed θ. The resulting conditions are not generally easy to satisfy.

Other effects can destroy perfect periodicity, which indicates the weakness of periodicity constraints. For example, as a consequence of the integrated Sachs-Wolfe effect, photons traveling along different paths will suffer different distortions, even if they originated in the same place. Likewise, any net lensing of the photon background will smear out periodicity.

The decay of the perturbation amplitude can have further consequences. The distribution of galaxies should also be affected [11]. Only small structures could form in the narrow part of the horn. The global topology may then create local inhomogeneity and distinctive patterns in the large-scale distribution of luminous and dark matter.

We have found that some topologies create strong effects on CBR sky maps in open universes. The periodicity scale for the horn topology we considered must exceed the size of the observable universe in order to hide the flat spots otherwise predicted in these maps. The horn configuration is a particular case, chosen to avoid chaotic nonintegrable geodesics, yet it is a good model of some characteristic features of complex identified topologies. In particular, the suppression of the power spectrum or features analogous to flat spots on the microwave sky will likely be more incisive in identifying topology than ghost images [14]. We have shown these attributes provide a sensitive probe of periodicity in the global topology of the Universe.

[1] A. Stebbins and R. R. Caldwell, Phys. Rev. D **52**, 3248 (1995).

[2] D. H. Lyth and A. Woszczyna, Phys. Rev. D **52**, 3338 (1995); J. Garcia-Bellido, A. R. Liddle, D. H. Lyth, and D. Wands, Phys. Rev. D **52**, 6750 (1995).

[3] K. Górski, B. Ratra, R. Stompor, N. Sugiyama, and A. J. Banday, Report No. astro-ph/9608054.

[4] M. White and J. Silk, Phys. Rev. Lett. **77**, 4704 (1996).

[5] D. D. Sokolov and V. F. Shvartsman, Sov. Phys. JETP **39**, 196 (1975); G. Paal, Acta. Phys. Acad. Sci. Hung. **30**, 51 (1971); J. R. Gott, Mon. Not. R. Astron. Soc. **193**, 153 (1980).

[6] I. Yu. Sokolov, JETP Lett. **57**, 617 (1993); A. de Oliveira-Costa and G. F. Smoot, Astrophys. J. **448**, 447 (1995).

[7] D. Stevens, D. Scott, and J. Silk, Phys. Rev. Lett. **71**, 20 (1993).

[8] A. A. Starobinsky, JETP Lett. **57**, 622 (1993); A. de Oliveira-Costa, G. F. Smoot, and A. A. Starobinsky, Astrophys. J. **468**, 457 (1996).

[9] N. L. Balazs and A. Voros, Phys. Rep. **143**, 109 (1986).

[10] N. J. Cornish, D. Spergel, and G. Starkman, Report No. gr-qc/9602039; N. J. Cornish, D. Spergel, and G. Starkman, Phys. Rev. Lett. **77**, 215 (1996).

[11] D. D. Sokolov and A. A. Starobinskii, Sov. Astron. **19**, 629 (1976).

[12] J. D. Barrow and J. Levin, Report No. astro-ph/9704041 [Phys. Lett. (to be published)].

[13] E. F. Bunn and M. White, Report No. astro-ph/9607060 [Astrophys. J. (to be published)].

[14] The proliferation of periodic orbits in the ergodic case of a compact pseudosphere might have the opposite effect of suppressing the power spectrum at small k. Still, if the complete basis of subcurvature modes are sufficient to describe a perturbation on a compact, open space then the exponential growth of long wavelength modes may not be relevant. This is a subtle issue worthy of further attention.